

Numerical evaluation of the Casimir interaction between cylinders

F.C. Lombardo ^{*}, F.D. Mazzitelli[†], and P.I. Villar [‡]

*Departamento de Física Juan José Giambiagi, FCEyN UBA, Facultad de Ciencias Exactas y Naturales,
Ciudad Universitaria, Pabellón I, 1428 Buenos Aires, Argentina*

(Dated: today)

We numerically evaluate the Casimir interaction energy for configurations involving two perfectly conducting eccentric cylinders and a cylinder in front of a plane. We consider in detail several special cases. For quasi-concentric cylinders, we analyze the convergence of a perturbative evaluation based on sparse matrices. For concentric cylinders, we obtain analytically the corrections to the proximity force approximation up to second order, and we present an improved numerical procedure to evaluate the interaction energy at very small distances. Finally, we consider the configuration of a cylinder in front of a plane. We first show numerically that, in the appropriate limit, the Casimir energy for this configuration can be obtained from that of two eccentric cylinders. Then we compute the interaction energy at small distances, and compare the numerical results with the analytic predictions for the first order corrections to the proximity force approximation.

PACS numbers: 12.20.Ds; 03.70.+k; 11.10.-z

I. INTRODUCTION

It has been 60 years since Casimir [1] found a profound explanation for the retarded van der Waals interaction as a manifestation of the zero-point energy of the quantum electromagnetic field. For many years the Casimir effect was little more than a theoretical curiosity. But interest in the phenomenon has blossomed in recent years. Experimental physicists have realized that the Casimir force affects the workings of micromachined devices, while advances in instrumentation have enabled the force to be measured with ever-greater accuracy. On theoretical grounds, considerable progress has also been achieved by studying the dependence of the Casimir force with the geometry of the conducting surfaces [2].

Up to now, most experiments aiming at a measurement of the Casimir force have been performed with parallel plates [3], or with a sphere in front of a plane [4]. The parallel plates configuration has a stronger signal, but the main experimental difficulty is to achieve parallelism between the plates. This problem is of course not present in the case of a sphere in front of a plane, but its drawback is that the force is several orders of magnitude smaller. The problem of the theoretical evaluation of the electromagnetic force for this configuration has been solved recently [5].

The configuration of two eccentric cylinders have both experimental and theoretical interest [6, 7]. Although parallelism is as difficult as for the plane-plane configuration, the fact that the concentric configuration is an unstable equilibrium position opens the possibility of measuring the derivative of the force using null experiments (for example, one could consider experimental configura-

tions in which a metallic wire is placed inside a larger hollow cylinder). The Casimir interaction energy between two eccentric cylindrical shells has been computed in [8], and was initially reported in [9]. Therein, it was used the mode summation technique combined with the argument theorem in order to write the Casimir energy as a contour integral in the complex plane, to end with an exact formula in which the vacuum energy is written in terms of the determinant of an infinite matrix. As a bonus, it has also been shown that the matrix elements in the general formula for two eccentric cylinders reproduce, as a limiting case of relevance, those of the Casimir energy for the cylinder-plane configuration. The latter geometry is also of experimental interest: being intermediate between the sphere-plane and the plane-plane geometries, it can shed some light on the longstanding controversy about thermal corrections to the Casimir force. Keeping the two plates parallel has proved very difficult, while the sphere and plate configuration avoids this problem, the force is not extensive. In the case of the cylinder-plane configuration, it is easier to hold the cylinder parallel and the force results extensive in its length. There is an ongoing experiment to measure the Casimir force for this configuration [10].

The aim of this paper is to provide a precise numerical evaluation of the analytical results obtained in [8]. The numerical evaluations will allow us to test different approximations, as the proximity force approximation (PFA) for close surfaces, and the "around the diagonal" approximation for quasi concentric cylinders. We will also show numerically that the energy of the eccentric cylinders configuration reproduces that of the cylinder-plane configuration, in the limit of very large eccentricity, when the radius of the external cylinder is also very large. Finally, we will present a detailed numerical evaluation for the vacuum energy for the cylinder-plane configuration, providing numerical support for the analytic predictions of the first order corrections to PFA [11].

The paper is organized as follows. In Section II we

*lombardo@df.uba.ar

†fmazzi@df.uba.ar

‡paula@df.uba.ar

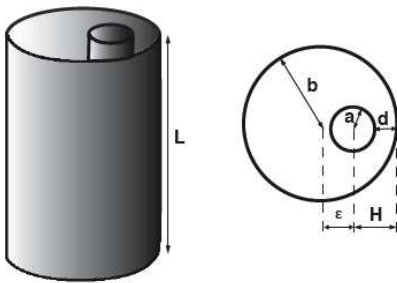


FIG. 1: Geometrical configuration for the eccentric cylinders. Two perfectly conducting cylinders of radii $a < b$, length $L \gg a, b$, and eccentricity ϵ interact via the Casimir force.

will discuss the general procedure used for the numerical evaluation of the Casimir energy in every case considered. In Section III, we will evaluate the exact formula for the interaction energy between eccentric cylinders. The complexity of the numerical evaluation increases as the radii of the cylinders get closer, and we provide details of the size of the matrices needed to assure convergence of the numerical results. In Section IV we analyze the particular case of quasi-concentric cylinders. We test the validity of the approximation developed in [8], based on tridiagonal matrices, that we extend to the next order by considering pentadiagonal matrices. In Section V we consider the particular case of concentric cylinders. We will obtain a new analytic result in the small distance limit, that includes the corrections to PFA up to the second order. We will also present an improved numerical method to evaluate the interaction energy at small distances. Finally, in section VI, we will numerically show that the interaction energy for the cylinder-plane configuration can be derived in the appropriate limit from the eccentric cylinders configuration, a result that was anticipated analytically for the matrix elements in [8]. In addition, we will evaluate numerically the cylinder-plane Casimir energy as the minimum distance between the surfaces is much smaller than the radius of the cylinder. We will be able to show numerically that the energy is well reproduced in this limit by the PFA, and to compute the first order correction to PFA for both TM and TE modes. In the first case (TM), the fits of the numerical data reproduce with high precision the analytic prediction [11]. On the other hand, the fits for TE modes are close to the analytic results or not, depending on the assumption about the higher order corrections.

II. NUMERICAL APPROACH

The evaluation of the Casimir interaction energy between two eccentric cylindrical shells (Fig.1) has been initially performed using PFA in Ref.[6]. However, it is possible to go beyond the PFA and find an exact formula for the interaction energy [8, 9]. This can be done using a mode by mode summation technique combined with

the argument theorem. By starting with the expression of the Casimir energy as $E = (\hbar/2) \sum_p (\omega_p - \tilde{\omega}_p)$, it has been shown in [8] that the Casimir interaction energy for two eccentric cylinders can be written as

$$\begin{aligned} E_{12} &= \frac{L}{4\pi a^2} \int_0^\infty d\beta \beta \ln(M(\beta)) \\ &= \frac{L}{4\pi a^2} \int_0^\infty d\beta \beta \left[\ln(M^{\text{TE}}(\beta)) + \ln(M^{\text{TM}}(\beta)) \right] \\ &= E^{\text{TE}} + E^{\text{TM}}, \end{aligned} \quad (1)$$

where $M^{\text{TM}}(\beta) = \det[\delta_{np} - A_{n,p}^{\text{TM}}]$ and $M^{\text{TE}}(\beta) = \det[\delta_{np} - A_{n,p}^{\text{TE}}]$. Here β is a dimensionless integration variable and n, p are arbitrary integers. Roughly speaking, the function M that determines the Casimir energy through Eq.(1) is such that its zeros give the eigenfrequencies of the geometric configuration. More precisely, it is the ratio of the function associated to the actual geometric configuration and the one associated to a configuration in which the conducting surfaces are very far away from each other [8]. The matrices $A_{n,p}^{\text{TM}}$ and $A_{n,p}^{\text{TE}}$ are defined as

$$A_{n,p}^{\text{TM}} = \frac{I_n(\beta)}{K_n(\beta)} \sum_m \frac{K_m(\alpha\beta)}{I_m(\alpha\beta)} I_{n-m} \left(\beta \frac{\epsilon}{a} \right) I_{p-m} \left(\beta \frac{\epsilon}{a} \right), \quad (2)$$

and similarly, for the TE modes, we have

$$A_{n,p}^{\text{TE}} = \frac{I'_n(\beta)}{K'_n(\beta)} \sum_m \frac{K'_m(\alpha\beta)}{I'_m(\alpha\beta)} I_{n-m} \left(\beta \frac{\epsilon}{a} \right) I_{p-m} \left(\beta \frac{\epsilon}{a} \right), \quad (3)$$

where $\alpha = b/a$ is the ratio between the outer and inner cylinder's radii and ϵ is the eccentricity (see Fig.1). I_n and K_n denote the modified Bessel functions.

In order to calculate the Casimir interaction energy, one needs to perform a numerical evaluation of the determinants in Eq.(1), followed by a numerical integration in the variable β . We find that as α approaches small values, larger matrices are needed for ensuring convergence. Likewise, as $\alpha \rightarrow 1$, the contribution to the integral is significant for a bigger integration range (bigger values of β contribute). That turns the problem into a real challenge from the numerical point of view. We numerically compute the Casimir interaction energy using a Fortran program. Once the M matrix elements for each configuration considered is defined, we use a standard routine to calculate its eigenvalues and determinant. Finally, we perform a standard integration over all values of β . The parameters used by the program are: the dimension of the M matrix (N,N), the number of addends m corresponding to each element of the M matrix, the integration limit (β_{max}) and the precision desired. The difficulty in running the programme lays in the compromise taken between all the parameters chosen.

In the following, we will evaluate the Casimir interaction energy for eccentric, quasi concentric, concentric cylinders, and also for the particular limit of a cylinder in front of a plane.

III. ECCENTRIC CYLINDERS

In this section, we present the numerical results for the Casimir interaction energy for two eccentric cylinders given by Eqs.(2) and (3).

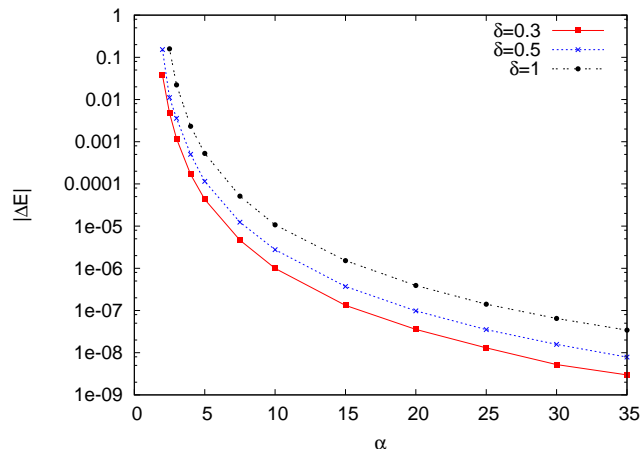


FIG. 2: Exact Casimir interaction energy difference $|\Delta E|$ between the eccentric and concentric configurations as a function of $\alpha = b/a$ for different values of $\delta = \epsilon/a$. Here $\Delta E = E_{12} - E_{12}^{cc}$. Energies are measured in units of $L/4\pi a^2$.

In Figs.2 and 3, we reproduce the exact Casimir interaction energy difference $\Delta E = E_{12} - E_{12}^{cc}$ between the eccentric and concentric configurations. In Fig.2 we plot the interaction energy difference $|\Delta E|$ as a function of α for different values of the eccentricity $\delta = \epsilon/a$. These numerical results interpolate between the PFA and the asymptotic behavior for large α [8]. In Fig.3 we show the Casimir interaction energy difference as a function of δ for various values of α . Again, it is evident that the equilibrium position ($\delta = 0$) is unstable.

In Refs.[8, 9] similar plots were performed using an algebraic evaluation of the trace of the matrix M , and a numerical integration, both using Mathematica. Due to this procedure, it was possible to evaluate the vacuum energy only for relatively large values of the parameter α , in order to reach convergence. With the numerical method we are presenting here, we are able to include smaller values of α , closer to the PFA region, where previous numerical calculations could not reach. Both in Fig.2 and Fig.3 we include runs for $\alpha > 1.75$. In order to achieve so, we have used matrices of dimension (21,21) and 501 addends in the sums of Eqs. (2) and (3) to assure convergence (variation smaller than 10^{-4}). For values $\alpha > 5$, smaller M matrices (5,5) can be used to obtain the plots with equal precision (indeed, as it was shown in [8], for $\alpha \rightarrow \infty$ the energy is dominated by the 00-element of the matrix M). The size of M for the runs was set by the smaller values of α that needed bigger M matrix to obtain the same accuracy.

The convergence of the numerical results depends both on the values of α and δ . For example, for $\alpha = 3$ and $\delta =$

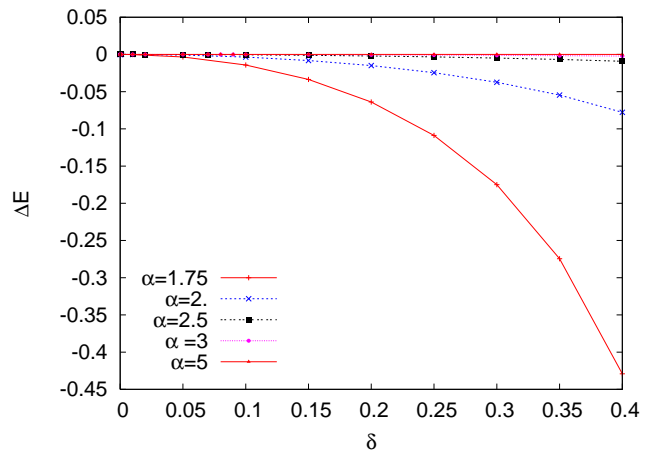


FIG. 3: Exact Casimir interaction energy difference ΔE between the eccentric and concentric configurations as a function of $\delta = \epsilon/a$ for different values of $\alpha = b/a$. Energies are measured in units of $L/4\pi a^2$. The maximum at $\delta = 0$ shows the instability of the concentric equilibrium position.

0.01 matrices (5,5) are enough, while for $\delta = 1$ matrices (9,9) are needed. In the case of $\alpha = 1.25$, it is necessary to use matrices of dimensions (55,55) and (101,101) when δ is 0.01 and 0.1, respectively.

IV. QUASI-CONCENTRIC CYLINDERS

In this section, we consider the situation in which the eccentricity of the configuration is much smaller than the radius of the inner cylinder ($\delta \ll 1$). For a small non-vanishing eccentricity, the behaviour of the Bessel functions in Eqs.(2) and (3) is $I_{m-n}(\beta\delta) \sim (\beta\delta)^{n-m}$ for small arguments. This suggests that the main contribution should be the one coming from the diagonal elements, and that one only needs to use matrix elements near the diagonal. We will test this idea through a numerical comparison between the Casimir interaction energy for different approximations and the exact energy derived in the previous section.

First order approximation. To begin with, we will only consider the matrix elements proportional to $I_0(\beta\delta)$, $I_1(\beta\delta)$ and $I_1^2(\beta\delta)$ as we are assuming small eccentricity $\delta = \epsilon/a \ll 1$. In this particular case, the M matrix become tridiagonal and the ϵ -dependent part of the Casimir energy will be quadratic in the eccentricity. We will describe in detail the case of the Dirichlet (TM) modes; the treatment of Neumann (TE) modes is similar. As was already mentioned in [8], to order $\mathcal{O}(\delta^2)$, the

non-vanishing elements of the matrix A_{np}^{TM} are:

$$\begin{aligned}
A_{n,n}^{\text{TM}(1)} &\simeq \frac{I_n(\beta)}{K_n(\beta)} \left[\frac{K_n(\alpha\beta)}{I_n(\alpha\beta)} I_0^2(\delta\beta) + \frac{K_{n-1}(\alpha\beta)}{I_{n-1}(\alpha\beta)} I_1^2(\delta\beta) \right. \\
&\quad \left. + \frac{K_{n+1}(\alpha\beta)}{I_{n+1}(\alpha\beta)} I_1^2(\delta\beta) \right], \\
A_{n,n+1}^{\text{TM}(1)} &\simeq \frac{I_n(\beta)}{K_n(\beta)} \left[\frac{K_n(\alpha\beta)}{I_n(\alpha\beta)} + \frac{K_{n+1}(\alpha\beta)}{I_{n+1}(\alpha\beta)} \right] I_0(\delta\beta) I_1(\delta\beta), \\
A_{n+1,n}^{\text{TM}(1)} &\simeq \frac{I_{n+1}(\beta)}{K_{n+1}(\beta)} \left[\frac{K_n(\alpha\beta)}{I_n(\alpha\beta)} + \frac{K_{n+1}(\alpha\beta)}{I_{n+1}(\alpha\beta)} \right] \\
&\quad \times I_0(\delta\beta) I_1(\delta\beta).
\end{aligned}$$

Second order approximation. In this case, we will consider that the main contribution to the Casimir interaction energy comes from the terms that contain up to $\mathcal{O}(\delta^4)$, extending the previous approximation to the next non trivial order. Then, the matrix A has additional non diagonal contributions, i.e. it is a pentadiagonal matrix with non-vanishing elements given by

$$\begin{aligned}
A_{n,n}^{\text{TM}(2)} &\simeq \frac{I_n(\beta)}{K_n(\beta)} \left[\frac{K_n(\alpha\beta)}{I_n(\alpha\beta)} I_0^2(\delta\beta) + \frac{K_{n-1}(\alpha\beta)}{I_{n-1}(\alpha\beta)} I_1^2(\delta\beta) \right. \\
&\quad + \frac{K_{n+1}(\alpha\beta)}{I_{n+1}(\alpha\beta)} I_1^2(\delta\beta) + \frac{K_{n-2}(\alpha\beta)}{I_{n-2}(\alpha\beta)} I_2^2(\delta\beta) \\
&\quad \left. + \frac{K_{n+2}(\alpha\beta)}{I_{n+2}(\alpha\beta)} I_2^2(\delta\beta) \right], \\
A_{n,n+1}^{\text{TM}(2)} &\simeq \frac{I_n(\beta)}{K_n(\beta)} \left[\frac{K_n(\alpha\beta)}{I_n(\alpha\beta)} + \frac{K_{n+1}(\alpha\beta)}{I_{n+1}(\alpha\beta)} \right] I_0(\delta\beta) I_1(\delta\beta), \\
A_{n+1,n}^{\text{TM}(2)} &\simeq \frac{I_{n+1}(\beta)}{K_{n+1}(\beta)} \left[\frac{K_n(\alpha\beta)}{I_n(\alpha\beta)} + \frac{K_{n+1}(\alpha\beta)}{I_{n+1}(\alpha\beta)} \right] \\
&\quad \times I_0(\delta\beta) I_1(\delta\beta), \\
A_{n,n+2}^{\text{TM}(2)} &\simeq \frac{I_n(\beta)}{K_n(\beta)} \left\{ \left[\frac{K_n(\alpha\beta)}{I_n(\alpha\beta)} + \frac{K_{n+2}(\alpha\beta)}{I_{n+2}(\alpha\beta)} \right] \right. \\
&\quad \times I_0(\delta\beta) I_2(\delta\beta) \\
&\quad \left. + \frac{K_{n+1}(\alpha\beta)}{I_{n+1}(\alpha\beta)} I_1^2(\delta\beta) \right\}, \\
A_{n+2,n}^{\text{TM}(2)} &\simeq \frac{I_{n+2}(\beta)}{K_{n+2}(\beta)} \left\{ \left[\frac{K_n(\alpha\beta)}{I_n(\alpha\beta)} + \frac{K_{n+2}(\alpha\beta)}{I_{n+2}(\alpha\beta)} \right] \right. \\
&\quad \times I_0(\delta\beta) I_2(\delta\beta) \\
&\quad \left. + \frac{K_{n+1}(\alpha\beta)}{I_{n+1}(\alpha\beta)} I_1^2(\delta\beta) \right\}.
\end{aligned}$$

In the following, we will numerically compare the Casimir interaction energy for the quasi concentric configuration computed using the first and second order approximations described above, with the one obtained using the exact formula given in Eqs.(2) and (3).

In Figs.4, 5 and 6 we present the Casimir interaction energy difference $\Delta E = E_{12} - E_{12}^{\text{cc}}$ between the eccentric and concentric configurations as a function of $\delta = \epsilon/a$ for different values of α . Therein, we can see the different curves corresponding to the exact energy difference (solid line) and the approximated ones obtained to first

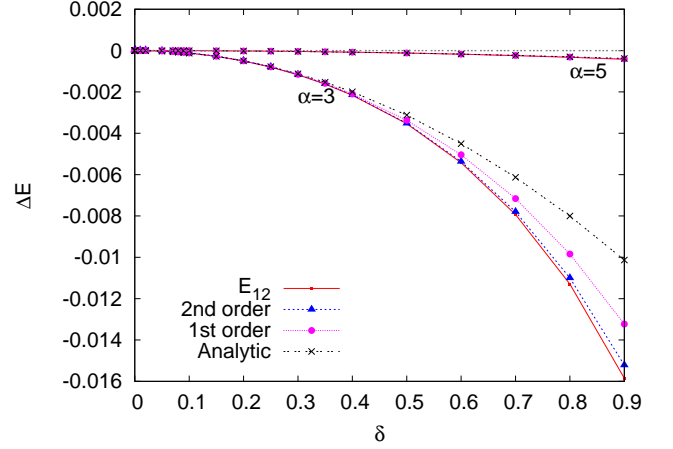


FIG. 4: Exact Casimir interaction energy difference ΔE between the eccentric and concentric configurations as a function of $\delta = \epsilon/a$ for different values of α . The solid line is the exact evaluation of the Casimir interaction energy, while the dashed line with triangles is the second order approximation and the dashed line with dots is the first order one. The analytic curve (dashed line with crosses) is the result of using Eq.(4). Energies are measured in units of $L/4\pi a^2$.

(dashed line with dots) and second order (dashed line with triangles) in the eccentricity. In all cases, matrix of dimension (21,21)[12] and 501 addends in the sums have been used to assure convergence.

We are also comparing the numerical results with the "analytic" result for quasi-concentric cylinders obtained Ref.[8]. Therein, it was shown that the determinant of the tridiagonal matrix can be explicitly evaluated up to quadratic order in δ , and therefore it was possible to write the interaction energy as a series

$$\begin{aligned}
E_{12}^{\text{TM}} &= E_{12}^{\text{TM,cc}} - \frac{L\epsilon^2}{4\pi a^4} \sum_n \int_0^\infty d\beta \beta^3 \frac{1}{1 - \mathcal{D}_{n,n}^{\text{TM,cc}}} \\
&\quad \times \left[\mathcal{D}_n^{\text{TM}} + \frac{\mathcal{N}_n^{\text{TM}}}{1 - \mathcal{D}_{n+1,n+1}^{\text{TM,cc}}} \right]. \quad (4)
\end{aligned}$$

Here

$$\begin{aligned}
\mathcal{D}_n^{\text{TM}} &\equiv \frac{\mathcal{D}_{n,n}^{\text{TM,cc}}}{2} + \frac{I_n(\beta)}{4K_n(\beta)} \left[\frac{K_{n-1}(\alpha\beta)}{I_{n-1}(\alpha\beta)} + \frac{K_{n+1}(\alpha\beta)}{I_{n+1}(\alpha\beta)} \right], \\
\mathcal{N}_n^{\text{TM}} &\equiv \frac{I_n(\beta)I_{n+1}(\beta)}{4K_n(\beta)K_{n+1}(\beta)} \left[\frac{K_n(\alpha\beta)}{I_n(\alpha\beta)} + \frac{K_{n+1}(\alpha\beta)}{I_{n+1}(\alpha\beta)} \right]^2, \\
\mathcal{D}_{n,n}^{\text{TM,cc}} &= \frac{I_n(\beta)}{K_n(\beta)} \frac{K_n(\alpha\beta)}{I_n(\alpha\beta)}. \quad (5)
\end{aligned}$$

The contribution of the TE modes to the interaction energy E_{12}^{TE} has a similar expression, replacing the Bessel functions by their derivatives with respect to the argument in the equations above. The numerical evaluation of this formulae in the plot is presented as the "analytic" curve.

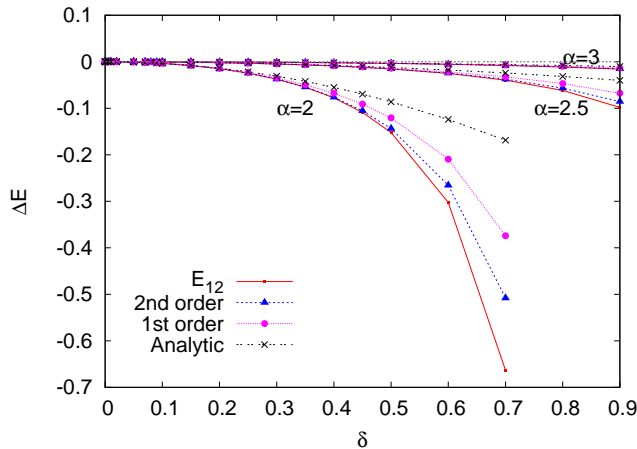


FIG. 5: Exact Casimir interaction energy difference ΔE between the eccentric and concentric configurations as a function of $\delta = \epsilon/a$ for different values of α . The solid line is the exact evaluation of the Casimir interaction energy, while the dashed line with triangles is the second order approximation and the dashed line with dots is the first order one. The analytic curve is the result of using Eq.(4). Energies are measured in units of $L/4\pi a^2$.

In Fig.4 we can see that the difference between several approximations increases with δ , for a given value of α . For example, for $\alpha = 5$ and $\delta = 0.5$, the analytic approximation differs from the exact result in 2%, and the first order approximation in 1%. For a larger value of δ , as $\delta = 0.9$, the differences are 9% and 4% for the analytic and first order approximations, respectively. The results for the second order approximation coincide with the exact result within the accuracy imposed. However, as the value of α becomes smaller, the differences become more visible. For $\alpha = 3$ the accuracy of the different approximations is, for $\delta = 0.5$, 12% (analytic), 5% (first order), and 0.6% (second order). On the other hand, for $\delta = 0.9$, we have 40% (analytic), 16% (first order), and 4% (second order).

In Fig.5 we present results for smaller values of α , and in Fig.6, we show a zoom-plot in order to appreciate better the differences.

In all cases considered, we can observe the expected hierarchy between the different approximations: while the second order approximation remains very similar to the exact result (within a 5% error) for $\alpha \geq 2$ and $\delta \leq 0.5$, the difference between the first order approximation and the exact result for $\alpha = 2$ and $\delta = 0.5$ is approximately 20%.

Taking into account that the different approximations are derived under the assumption $\delta \ll 1$, the validity of the approximate results is, in general, better than expected. Moreover, the results of this section show that the combination of analytic and numerical results allow a much more efficient numerical evaluation of the Casimir energy. In the particular case considered here (quasi concentric cylinders), from the numerical point of view it is

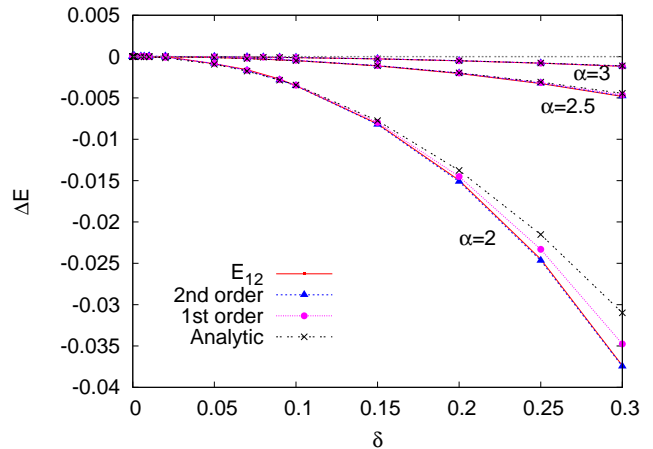


FIG. 6: Exact Casimir interaction energy difference ΔE between the eccentric and concentric configurations as a function of $\delta = \epsilon/a$ for different values of α (a smaller range of δ). The solid line is the exact evaluation of the Casimir interaction energy, while the dashed line with triangles is the second order approximation and the dashed line with dots is the first order one. The analytic curve (dashed line with crosses) is the result of using Eq.(4). Energies are measured in units of $L/4\pi a^2$.

much more convenient to consider sparse matrices concentrated on the diagonal, than large matrices in which all elements are non vanishing.

V. CONCENTRIC CYLINDERS

In this section we will derive an analytic result for the vacuum energy in the concentric cylinders configuration valid for small distances, beyond PFA, and we will present an improved numerical method to evaluate the interaction energy at small distances for the particular case of two concentric cylinders.

The exact formula for eccentric cylinders coincides, of course, with the known result for the Casimir energy for concentric cylinders ($\epsilon = 0$). Indeed, as $I_{n-m}(0) = \delta_{nm}$, in this particular case the matrices $A_{np}^{\text{TE},\text{TM}}$ become diagonal and the exact formula reduces to [8, 13]:

$$E_{12}^{\text{cc}} = \frac{L}{4\pi a^2} \int_0^\infty d\beta \beta \ln M^{\text{cc}}(\beta), \quad (6)$$

where

$$M^{\text{cc}}(\beta) = \prod_n \left[1 - \frac{I_n(\beta)K_n(\alpha\beta)}{I_n(\alpha\beta)K_n(\beta)} \right] \left[1 - \frac{I'_n(\beta)K'_n(\alpha\beta)}{I'_n(\alpha\beta)K'_n(\beta)} \right]. \quad (7)$$

The first factor corresponds to Dirichlet (TM) modes and the second one to Neumann (TE) modes. The concentric-cylinders configuration is interesting from a theoretical point of view, since it can be used to test analytic and numerical methods. It also has potential implications for the physics of nanotubes [9, 14].

The proximity limit $\alpha - 1 \ll 1$ has already been analyzed for the concentric case [13]. In order to compute the Casimir energy in this limit, it was necessary to use the uniform expansion of the Bessel functions and to perform a summation over all values of n . As expected, the result is equal to the one obtained via the proximity approximation, namely

$$E_{12, PFA}^{\text{TE,cc}} = E_{12, PFA}^{\text{TM,cc}} = \frac{1}{2} E_{12, PFA}^{\text{EM,cc}} = -\frac{\pi^3 L}{720 a^2} \frac{1}{(\alpha - 1)^3}, \quad (8)$$

and both TE and TM modes contribute with the same weight to the total energy.

A. Beyond proximity approximation: the next to next to leading order

We will now compute analytic corrections to the PFA given in Eq.(8). Due to the simplicity of this configuration, we will be able to obtain not only the next to leading order, but also the next to next to leading contribution. In order to do that, we need the uniform expansions of the Bessel functions. We have

$$\frac{I_n(ny)K_n(n\alpha y)}{I_n(n\alpha y)K_n(ny)} = \frac{(1 - \frac{u(t_\alpha)}{n})(1 + \frac{u(t_1)}{n})}{(1 - \frac{u(t_1)}{n})(1 + \frac{u(t_\alpha)}{n})} e^{-2n[\eta(\alpha y) - \eta(y)]}, \quad (9)$$

and

$$\frac{I'_n(ny)K'_n(n\alpha y)}{I'_n(n\alpha y)K'_n(ny)} = \frac{(1 - \frac{v(t_\alpha)}{n})(1 + \frac{v(t_1)}{n})}{(1 - \frac{v(t_1)}{n})(1 + \frac{v(t_\alpha)}{n})} e^{-2n[\eta(\alpha y) - \eta(y)]}, \quad (10)$$

where

$$\begin{aligned} \eta(y) &= \sqrt{1+y^2} + \ln \frac{y}{1 + \sqrt{1+y^2}}; \\ u(t) &= \frac{3t - 5t^3}{24}; \quad t_\alpha = \frac{1}{\sqrt{1 + \alpha^2 y^2}}, \\ v(t) &= \frac{7t^3 - 9t}{24}. \end{aligned} \quad (11)$$

With these expansions at hand, we can evaluate the matrix M both for the TE and TM modes. The expression in Eq. (7) can be approximated by

$$M^{cc} \approx \left(1 - e^{-2n\Delta\eta(y)} A(n, y)\right) \left(1 - e^{-2n\Delta\eta(y)} B(n, y)\right), \quad (12)$$

where

$$\Delta\eta(y) = h(y)(\alpha - 1) - \frac{(\alpha - 1)^2}{2h(y)} + \frac{(2 + 3y^2)}{6h(y)^3} (\alpha - 1)^3, \quad (13)$$

with $h(y) = \sqrt{1+y^2}$. In Eq.(12) we have defined coefficients $A(n, y)$ and $B(n, y)$ in terms of the expansions of

the functions $u(t)$ and $v(t)$. They read

$$\begin{aligned} A(n, y) &= 1 + (\alpha - 1) \frac{y^2 (6 + 7y^2 + y^4)}{4n (1 + y^2)^{\frac{7}{2}}}, \\ B(n, y) &= 1 - (\alpha - 1) \frac{y^2 (-4 + 37y^2)}{4n (1 + y^2)^{\frac{5}{2}}}. \end{aligned} \quad (14)$$

Replacing Eq.(12) into Eq.(6), and expanding the logarithm as a series, it is possible to compute explicitly the remaining integrals in β . After a long calculation, the Casimir energy can be written as

$$\begin{aligned} E_{12}^{cc} &\approx -\frac{\pi^3 L}{360 a^2 (\alpha - 1)^3} \left\{ 1 + \left(\frac{1}{4} + \frac{1}{4}\right)(\alpha - 1) \right. \\ &\quad \left. - \left(\frac{1}{\pi^2} + \frac{1}{\pi^2} + \frac{1}{10}\right)(\alpha - 1)^2 + \dots \right\}. \end{aligned} \quad (15)$$

In the expression above, the first term inside the parenthesis corresponds to the proximity approximation contribution given in Eq.(8), while the second and third terms are the first and second order corrections, respectively. It is worth noticing that the sub-leading term coincides with the result obtained by means of the semiclassical approximation [13]. It is also important to remark that both TM and TE modes contribute with the same weight to the energy in the leading and the next to leading orders. However, this is not the case in the quadratic term. There is a factor $1/\pi^2$ coming from the TM mode, and a factor $1/\pi^2 + 1/10$ corresponding to the TE one.

B. Improving the convergence of the numerical evaluation

Numerical calculations of the Casimir energy for α very close to one are very difficult since big number of terms have to be considered in the sums, and therefore convergence problems arise, mainly produced by underflows and overflows in the evaluation of Bessel functions of large orders.

In order to perform a numerical evaluation of the Casimir energy in the proximity region, we will describe a subtraction method, in which we have used the value of the energy in the PFA to improve the numerics [15].

In the case we are concerned here, we can add and subtract the interaction energy for concentric cylinders computed using the leading uniform asymptotic expansion for the Bessel functions, up to first order in $\alpha - 1$:

$$\begin{aligned} \frac{K_n(n\alpha y)}{K_n(ny)} \frac{I_n(ny)}{I_n(n\alpha y)} &\simeq \frac{K'_n(n\alpha y)}{K'_n(ny)} \frac{I'_n(ny)}{I'_n(n\alpha y)} \\ &\simeq e^{-2n(\alpha - 1)\sqrt{1+y^2}}. \end{aligned} \quad (16)$$

We denote by \tilde{E} the interaction energy obtained by inserting these expansions into Eq. (6), which can be com-

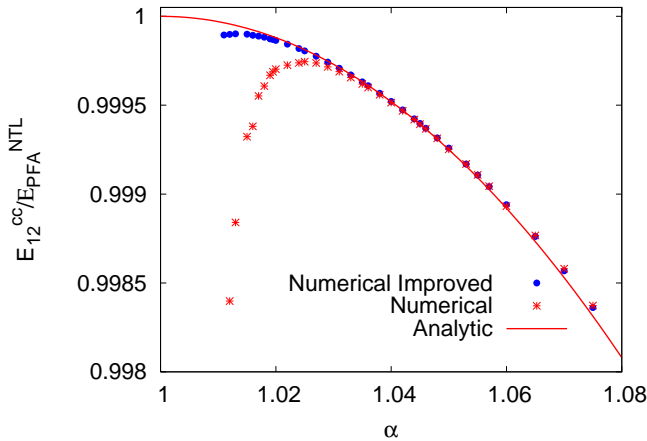


FIG. 7: Ratio between the exact Casimir energy for concentric cylinders E_{12}^{cc} and the Casimir energy estimated using the PFA up to the next to leading order E_{PFA}^{NTL} , as a function of the parameter α . This is done for two different methods: the numerical (of slow convergence) and the numerical improved (subtraction method).

puted analytically

$$\tilde{E} = -\frac{1}{2(\alpha-1)^2} \sum_{k \geq 1} \frac{1}{k^3} \frac{1}{(e^{2k(\alpha-1)} - 1)} \times \left[1 + \frac{2k(\alpha-1)e^{2k(\alpha-1)}}{(e^{2k(\alpha-1)} - 1)} \right], \quad (17)$$

and contains the leading order of the Casimir energy. Now we write

$$E_{12}^{cc} = (E_{12}^{cc} - \tilde{E}) + \tilde{E}. \quad (18)$$

The difference contained in the brackets in Eq. (18), has a faster convergence than the original sum and, therefore, can be easily calculated numerically.

In Fig.7 we present both Casimir energy of the concentric cylinders for the direct numerical calculation (of slow convergence) and the alternative method mentioned above. In this figure we plot the ratio $E_{12}^{cc}/E_{PFA}^{NTL}$ where

$$E_{PFA}^{NTL} = -\frac{\pi^3 L}{360a^2(\alpha-1)^3} \left\{ 1 + \frac{1}{2}(\alpha-1) \right\}. \quad (19)$$

As can be seen, with this subtraction method it is possible to compute the exact energy for values of α much closer to 1, while the accuracy of the direct calculation is worse for $\alpha < 1.02$. Moreover, the numerical results confirm the analytic result given in Eq.(15). We have fit the ratio between the Casimir interaction energy with the next to leading correction of Eq.(19), $E_{12}^{cc}/E_{PFA}^{NTL} = a + b(\alpha-1)^2$, obtaining $a = 1.00$, and $b = 0.29$. The analytical results, expected from Eqs.(15) and (19) are $a = 1$ and $b = 0.3026$, which means that we are checking the next to next leading correction with an error smaller than 1.5%.

A similar method could in principle be applied to the eccentric cylinders or the cylinder-plane configurations, although in these cases the main difficulty is the analytic evaluation of the approximate energy that has to be added and subtracted.

VI. A CYLINDER IN FRONT OF A PLANE

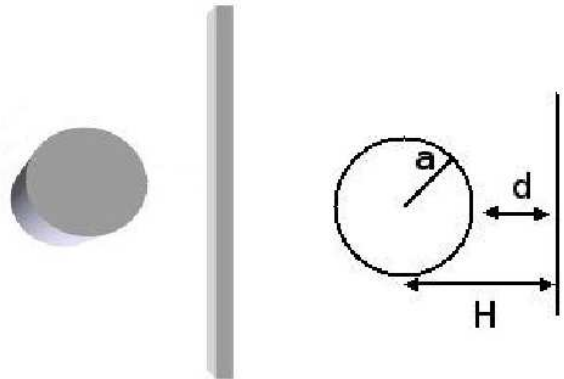


FIG. 8: Cylinder-plane configuration. A perfectly conducting cylinder of radius a is in front of a perfectly conducting plane at a distance d .

In this section, we will study the cylinder-plane configuration (Fig.8). The Casimir energy for this configuration was first evaluated in the PFA in Ref.[6]. The exact formula has been derived in Refs.[11, 16], and has the same structure than Eq.(1), but with the matrix elements $A_{n,p}^{TE}$ and $A_{n,p}^{TM}$ replaced by the corresponding ones for this geometry, that we will denote by $A_{n,p}^{TE,CP}$ and $A_{n,p}^{TM,CP}$.

As suggested by simple geometric arguments, the eccentric cylinders formula reproduces the cylinder-plane matrix elements in the limit $b, \epsilon \rightarrow \infty$, keeping $H = b - \epsilon$ fixed. Indeed, using the uniform expansion of the Bessel functions, and as explained in Ref.[8], the matrix elements $A_{n,p}^{TE}$ and $A_{n,p}^{TM}$, become respectively,

$$A_{n,p}^{TE} \simeq -\frac{I'_n(\beta)}{K'_n(\beta)} K_{n+p}(2\beta H/a) \equiv A_{n,p}^{TE,CP}, \quad (20)$$

and

$$A_{n,p}^{TM} \simeq \frac{I_n(\beta)}{K_n(\beta)} K_{n+p}(2\beta H/a) \equiv A_{n,p}^{TM,CP}. \quad (21)$$

These expressions coincide with the result for the TE and TM modes in the cylinder plane configuration [11, 16].

In the following we will, firstly, compare the exact Casimir interaction energy for the cylinder-plane configuration with that of the two eccentric cylinders, in the limit that the latter reproduces the former configuration.

In the end of the section, we will numerically evaluate the cylinder plane Casimir for small distances, in order to discuss the leading correction to the PFA.

A. Comparison between eccentric cylinders and cylinder-plane configurations

We will now show explicitly that the numerical evaluation of the vacuum energy for eccentric cylinders, based on Eqs.(1,2) and (3), reproduce the exact results for the cylinder-plane configuration, described by Eq.(1) with the matrix elements given by Eqs.(20) and (21).

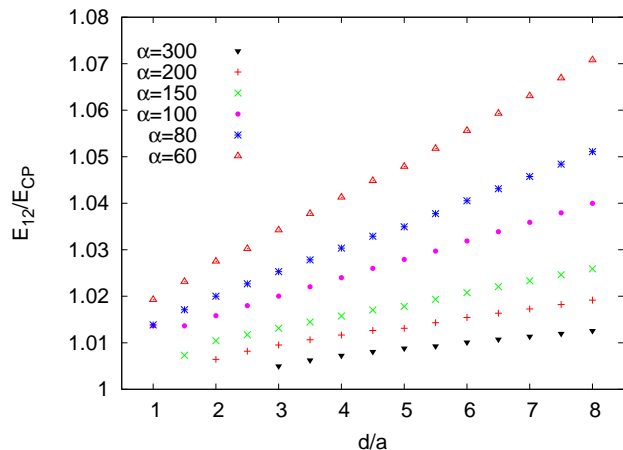


FIG. 9: Comparison between the exact Casimir interaction energy for eccentric cylinders and the cylinder-plane configuration as a function of $d = H - a$ for different values of α .

In Fig.9 we present the ratio of both energies as a function of d for different values of α . These runs were done by the use of matrices of dimension (81, 81) and 901 addends in the sums of Eqs.(2) and (3). The need of big matrices is set by the cylinder-plane configuration program, while the number of addends is set by the eccentric cylinders geometry. From the numerical results we see that, as expected, the vacuum energy of the eccentric cylinders tends to the vacuum energy of the cylinder in front of a plane for large values of b and ϵ , when H and a are fixed. The coincidence is of course better for smaller values of d , the minimum distance between surfaces.

In all cases, we can see that the exact Casimir interaction for eccentric cylinders is bigger than the cylinder plane energy. This result is expected from the PFA, since the conducting surfaces are closer to each other in the case of the two eccentric cylinders than in the cylinder-plane configuration, for a given minimum distance between surfaces.

B. Numerical evaluation of the cylinder-plane Casimir energy beyond the Proximity Force Approximation

In this section we present a detailed computation of the vacuum energy for the cylinder-plane configuration. In Fig.10 we present the Casimir interaction energy for the cylinder-plane configuration obtained by the use of our Fortran program. For the runs, we used a matrix of dimension (101,101) to reach the proximity area ($d \rightarrow 0$). It must be mentioned that for smaller values of d , we need to increase the dimension of the A matrix and the integration range of β in Eq.(1). This fact becomes our major limitation to reach yet smaller values of d .

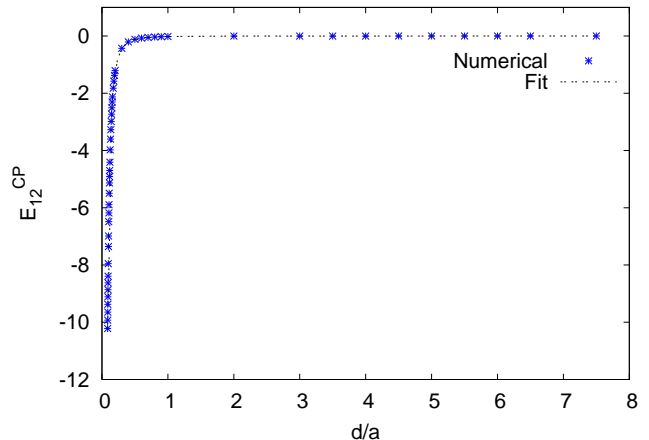


FIG. 10: Leading term for the Casimir interaction energy of the cylinder-plane configuration. The leading term behaves proportional to $-0.0228 d^{-5/2}$. A simple fit $f(x) = \gamma x^\zeta$ of the numerical data for $d/a < 1$ gives $\gamma = -0.021$ and $\zeta = -2.53$.

We now discuss in more detail the limit $d \ll a$. This problem has been considered from an analytical point of view in Ref.[11]. Using the uniform expansions for the Bessel functions appearing in the matrix elements $A_{n,p}^{\text{TE,CP}}$ and $A_{n,p}^{\text{TE,CP}}$, and after complex calculations, it can be shown that, in the proximity limit:

$$E_{\text{CP}}^{\text{TM}} = -\frac{1}{2\pi} \sqrt{\frac{a}{d^5}} \frac{3\zeta(4)}{32\sqrt{2}} \left(1 + 0.1944 \frac{d}{a} + \dots \right), \quad (22)$$

$$E_{\text{CP}}^{\text{TE}} = -\frac{1}{2\pi} \sqrt{\frac{a}{d^5}} \frac{3\zeta(4)}{32\sqrt{2}} \left(1 - 1.1565 \frac{d}{a} + \dots \right), \quad (23)$$

where we have written separately the contributions of TM and TE modes.

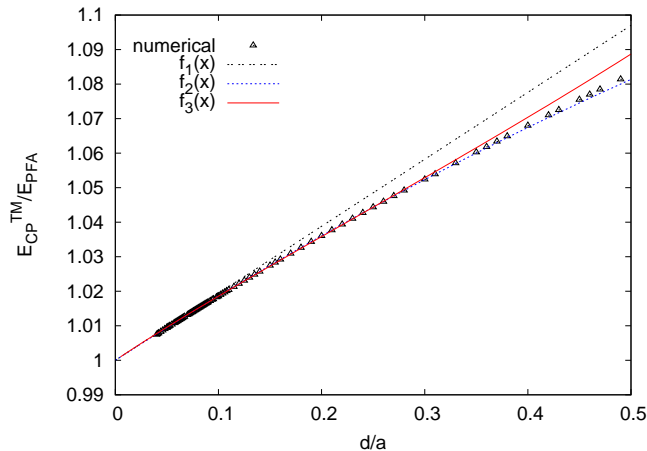


FIG. 11: Numerical result for the TM modes for the cylinder-plane configuration, and the corresponding fits presented in Table I. A simple linear fit $f(x) = a + bx$ of the numerical data in the interval $0.04 \leq d/a \leq 0.07$ gives $a = 0.9999$ and $b = 0.1900$. The theoretical values are $a = 1$ and $b = 0.1944$.

d/a	$f_1(x) = 1 + bx$	$f_2(x) = 1 + b * x + c * x^2$	$f_3(x) = 1 + b * x + c * x^2 * \log(x)$
[0.04 : 0.15]	$b = 0.1864$	$b = 0.1922, c = -0.0601$	$b = 0.1961, c = 0.0438$
[0.04 : 0.20]	$b = 0.1849$	$b = 0.1923, c = -0.0613$	$b = 0.1983, c = 0.0540$
[0.04 : 0.25]	$b = 0.1829$	$b = 0.1922, c = -0.0601$	$b = 0.2003, c = 0.0634$
[0.04 : 0.30]	$b = 0.1811$	$b = 0.1920, c = -0.0586$	$b = 0.2022, c = 0.0716$
[0.04 : 0.35]	$b = 0.1794$	$b = 0.1918, c = -0.0572$	$b = 0.2045, c = 0.0810$
[0.04 : 0.40]	$b = 0.1771$	$b = 0.1914, c = -0.0549$	$b = 0.2076, c = 0.0935$

TABLE I: Different fits for the numerical results of Fig. 11. We fix $f_i(0) = 1$ since the numerical data agree this value with high precision.

d/a	$f_1(x) = 1 + bx$	$f_2(x) = 1 + b * x + c * x^2$	$f_3(x) = 1 + b * x + c * x^2 * \log(x)$
[0.04 : 0.15]	$b = -0.8301$	$b = -0.9704, c = 1.4499$	$b = -1.0711, c = -1.0852$
[0.04 : 0.20]	$b = -0.8013$	$b = -0.9509, c = 1.2326$	$b = -1.0772, c = -1.1141$
[0.04 : 0.25]	$b = -0.7683$	$b = -0.9349, c = 1.0794$	$b = -1.0890, c = -1.1674$
[0.04 : 0.30]	$b = -0.7399$	$b = -0.9222, c = 0.9772$	$b = -1.1037, c = -1.2306$
[0.04 : 0.35]	$b = -0.7158$	$b = -0.9091, c = 0.8879$	$b = -1.1232, c = -1.3115$
[0.04 : 0.40]	$b = -0.6851$	$b = -0.8943, c = 0.7999$	$b = -1.1534, c = -1.4360$

TABLE II: Different fits for the numerical results of Fig. 12. We fix $f_i(0) = 1$ since the numerical data agree this value with high precision.

We will discuss the first order corrections to PFA for TM and TE modes separately. In Fig.11, we show our numerical results for the TM modes. The fit of the numerical results depends of course on the interval chosen for d/a . There is an obvious compromise: on the one hand, as already mentioned, we cannot consider very small values for d/a because of numerical limitations. On the other hand, the expansion in powers of d/a are expected to be valid only for $d/a \ll 1$. In any case, as can be seen from Table I, the different fits for the numerical results are stable, and confirm both the PFA to leading and next to leading orders. Indeed, the results are fully compati-

ble with the analytic results given in Eq.(22), considering both linear and quadratic fits of the numerical results. Moreover, a simple linear fit in a smaller range of d/a gives $a = 0.9999$ and $b = 0.1900$ and already reproduces the analytical results [11] with high accuracy (see also numerical findings in [17]).

In Fig.12, we show our results for the Neumann modes, and we include in Table II different fits of the numerical data. In this case, the value obtained for the linear correction to PFA depends strongly on the assumption about the next non trivial correction. This is not surprising: as we cannot consider extremely small values for

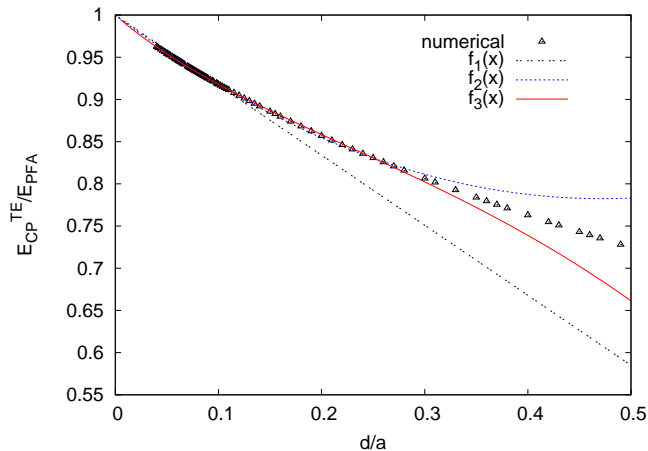


FIG. 12: Numerical result for the TE modes for the cylinder-plane configuration, and the corresponding fits presented in Table II. A simple linear fit $f(x) = a + bx$ of the numerical data in the interval $0.04 \leq d/a \leq 0.07$ gives $a = 0.9940$ and $b = -0.7808$. The theoretical values are $a = 1$ and $b = -1.1565$.

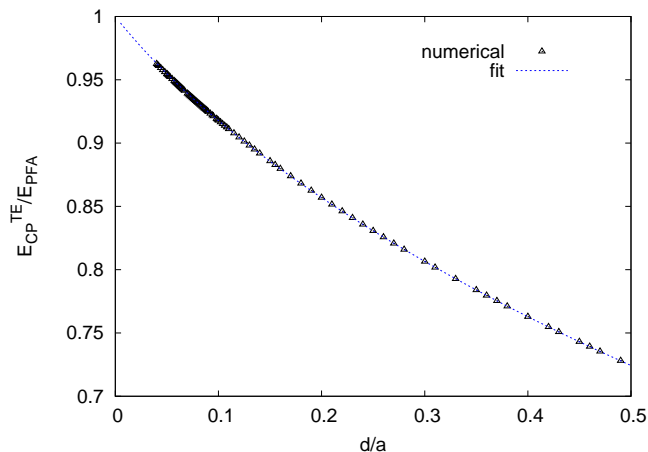


FIG. 13: A numerical fit of the results for the TE modes including cubic corrections $f(x) = 1 + bx + cx^2 \log x + dx^3$. The coefficients are $b = -1.0478$, $c = -0.9485$, and $d = 0.6708$.

d/a , the non linear corrections may have a non negligible contribution in the intervals chosen for the fits. For example, a simple linear fit gives $a = 0.994$ and $b = -0.7808$ which does not coincide with the result in Eq.(23). However, based on the discussion about the slower convergence of the Neumann corrections presented in Ref.[11], we have allowed the possibility of non linear corrections proportional to $(d/a)^2 \ln(d/a)$ in our fits. Remarkably, when this non linear corrections are taken into account, the coefficient of the linear correction gets closer to the analytic prediction in Eq.(23), that we reproduce with an error less than 7%. Note that, as can be seen in Fig.11,

this is not the case for TM modes, since the best fit of the numerical data contains a quadratic term without a logarithm. In Fig.13 we show a fit of the numerical data for TM modes that includes a cubic correction $(d/a)^3$. With this additional term, the fit reproduces the numerical data up to $d/a = 0.5$.

To summarize, the fits of the numerical data clearly confirm the analytic prediction for the TM modes, and suggest that the next non trivial correction for the TE modes is not quadratic but proportional to $(d/a)^2 \ln(d/a)$.

VII. FINAL REMARKS

We have numerically evaluated the Casimir interaction energy for the two eccentric cylinders configuration and for the cylinder plane geometry, extending in several directions the numerical results presented in Ref.[8]. For quasi concentric cylinders, we have shown that the approximation based on tridiagonal matrices derived in [8] is in good agreement with the numerical values. We also extended this approximation to the case of pentadiagonal matrices. Our results show that, for small eccentricities, it is far more efficient to consider the contribution of the matrix elements near the diagonal, than a "tour de force" numerical calculation based on the exact formula.

For concentric cylinders, we have obtained analytically the quadratic corrections to the PFA. As far as we know, this is the first explicit non linear correction to PFA existing in the literature. We have also shown that the PFA can be used as a useful tool in order to improve the numerical evaluation at very small distances, and we have used this improvement in order to check numerically the non linear correction to PFA.

Finally, we have analyzed in detail some numerical results for the cylinder-plane geometry. On the one hand, we have shown that the Casimir energy for this configuration can be obtained from that of the two eccentric cylinders. Although this coincidence has been anticipated for the matrix elements in Ref.[8], the numerical data show that the result is also valid for the energy. On the other hand, we have computed the TE and TM contributions to the energy for small distances, and compared the fits of the numerical results with existing analytic predictions for the linear corrections to the PFA.

Acknowledgments

This work has been supported by CONICET, UBA and ANPCyT, Argentina. We would like to thank M. Bordag for useful comments.

-
- [1] H.B.G. Casimir, Proc. K. Ned. Akad. Wet. B 51, 793 (1948).
- [2] G. Plunien, B. Muller, and W. Greiner, Phys. Rep. **134**, 87 (1986); P. Milonni, *The Quantum Vacuum* (Academic Press, San Diego, 1994); V. M. Mostepanenko and N. N. Trunov, *The Casimir Effect and its Applications* (Clarendon, London, 1997); M. Bordag, *The Casimir Effect 50 Years Later* (World Scientific, Singapore, 1999); M. Bordag, U. Mohideen, and V.M. Mostepanenko, Phys. Rep. **353**, 1 (2001); K. A. Milton, *The Casimir Effect: Physical Manifestations of the Zero-Point Energy* (World Scientific, Singapore, 2001); S. Reynaud et al., C. R. Acad. Sci. Paris IV-2, 1287 (2001); K. A. Milton, J. Phys. A: Math. Gen. 37, R209 (2004); S.K. Lamoreaux, Rep. Prog. Phys. **68**, 201 (2005).
- [3] G. Bressi, G. Carugno, R. Onofrio, and G. Ruoso, Phys. Rev. Lett. **88**, 041804 (2002).
- [4] S.K. Lamoreaux, Phys. Rev. Lett. **78**, 5 (1997); U. Mohideen and A. Roy, Phys. Rev. Lett. **81**, 4549 (1998); B.W. Harris, F. Chen, and U. Mohideen, Phys. Rev. A **62**, 052109 (2000); T. Ederth, Phys. Rev. A **62**, 062104 (2000); H.B. Chan, V.A. Aksyuk, R.N. Kleiman, D.J. Bishop, and F. Capasso, Science 291, 1941 (2001); H. B. Chan, V.A. Aksyuk, R.N. Kleiman, D.J. Bishop, and F. Capasso, Phys. Rev. Lett. **87**, 211801 (2001); G. Bressi, G. Carugno, R. Onofrio, and G. Ruoso, Phys. Rev. Lett. **88**, 041804 (2002); D. Iannuzzi, I. Gelfand, M. Lisanti, and F. Capasso, Proc. Nat. Ac. Sci. USA 101, 4019 (2004); R.S. Decca, D. Lopez, E. Fischbach, and D.E. Krause, Phys. Rev. Lett. **91**, 050402 (2003); R.S. Decca et al., Phys. Rev. Lett. **94**, 240401 (2005); R.S. Decca et al., Annals of Physics **318**, 37 (2005).
- [5] T. Emig, J. Stat. Mech., P04007 (2008); P. A. Maia Neto, A. Lambrecht, S. Reynaud, Phys. Rev. A **78**, 012115 (2008). The case of a scalar field with Dirichlet boundary conditions has been discussed in H. Gies and K. Klingmüller, Phys. Rev. Lett. **96**, 220401 (2006); A. Bulgac, P. Magierski, and A. Wirzba, Phys. Rev. D **73**, 025007 (2006).
- [6] D.A.R. Dalvit, F.C. Lombardo, F.D. Mazzitelli, and R. Onofrio, Europhys. Lett. **68**, 517 (2004).
- [7] F.D. Mazzitelli, in *Quantum Field Theory Under the Influence of External Conditions*, K.A. Milton (editor), Rinton Press, Princeton (2004).
- [8] F.D. Mazzitelli, D.A.R. Dalvit and F.C. Lombardo, New Journal of Physics **8**, 240 (2006).
- [9] D.A.R. Dalvit, F.C. Lombardo, F.D. Mazzitelli, and R. Onofrio, Phys. Rev. A **74**, 020101 (2006).
- [10] M. Brown-Hayes, D.A.R. Dalvit, F.D. Mazzitelli, W.J. Kim, and R. Onofrio, Phys. Rev. A **72**, 052102 (2005).
- [11] M. Bordag, Phys. Rev. D **73**, 025007 (2006).
- [12] We are using different programs to simulate the different situations such as the eccentric cylinders, quasi concentric to first order and quasi concentric to second order. As we have to assure convergence in each of them, that is why we have used bigger matrix than before.
- [13] F. D. Mazzitelli, M. J. Sánchez, N. N. Scoccola and J. von Stecher, Phys. Rev. A **67**, 013807 (2003).
- [14] E.V. Blagov, G.L. Klimchitskaya, and V.M. Mostepanenko, Phys. Rev. B **71**, 235401 (2005).
- [15] F.C. Lombardo, F.D. Mazzitelli, and P.I. Villar, J. Phys. A **41**, 164009 (2008).
- [16] T. Emig, R.J. Jaffe, M. Kardar and A. Scardicchio, Phys. Rev. Lett. **96**, 080403 (2006). See also S. J. Rahi, A. W. Rodriguez, T. Emig, R.L. Jaffe, S.G. Johnson and M. Kardar, Phys. Rev. A **77**, 030101(R) (2008); S.J. Rahi, T. Emig, R.L. Jaffe, and M. Kardar, Phys. Rev. A **78**, 012104 (2008).
- [17] H. Gies and K. Klingmüller, Phys. Rev. D **74**, 045002 (2006).